JAERI-Research
94-030

STABILITY ANALYSIS OF ITER PLASMAS WITH H-MODE PROFILES

November 1994

Shinji TOKUDA and Takahisa OZEKI

日本原子力研究所
Japan Atomic Energy Research Institute

編集兼発行　日本原子力研究所
印　　刷　㈱原子力資料サービス

Stability Analysis of ITER Plasmas with H－mode Profiles

Shinji TOKUDA and Takahisa OZEKI

Department of Fusion Plasma Research
Naka Fusion Research Establishment
Japan Atomic Energy Research Institute
Naka-machi, Naka-gun, Ibaraki-ken

(Received October 5, 1994)

The ideal MHD stability properties of ITER TAC-4 H-mode profiles are studied. The effects of the current profile variation on the stability of high-n ballooning modes and the n=1 mode are analyzed (n: toroidal mode number). The variation of the current profile is characterized by the change of the safety factor on the magnetic axis, q_0, while the total plasma current is fixed. The beta limit of the high-n ballooning modes remains $g_T = 3.3$ for such variations (g_T :Troyon's factor). The unstable n=1 mode is strongly localized at the plasma edge (peeling mode) for $q_0 = 1.0$ and the beta limit of the n = 1 mode is $g_T = 3.7$. In case of $q_0 < 0.9$, the stability of the n = 1 mode is determined by the internal kink mode and the beta limit is reduced to $g_T = 2.4$ for $q_0 = 0.8$. Stability analysis predicts that the H－mode profiles with $g_T = 3$ can be realized when q_0 is kept to be greater than 0.9 and the current profile at the edge is fixed. This analysis also shows the stability of the TAC4 H-mode profiles will be sensitive to the edge current profile.

Keywords : Tokamak, MHD Stability, Beta Limit, High-n Ballooning Mode, Peeling Mode, Internal Kink Mode, H-mode, ITER Physics R&D

ＩＴＥＲ Ｈ－モード分布プラズマの安定性解析

日本原子力研究所那珂研究所炉心プラズマ研究部
徳田 伸二・小関 隆久

（1994年10月5日受理）

ＩＴＥＲ ＴＡＣ－４ Ｈ－モード分布の持つ理想ＭＨＤ安定性の性質を調べた。主として，電流分布の変化が高－ｎバルーニング・モードおよびｎ＝１モードの安定性に与える影響を解析した（ｎ：トロイダル・モード数）。電流分布の変化は磁気軸上の安全係数の変化で特徴づけられ，このとき，全プラズマ電流は一定値に保たれる。このような変化に対して，高－ｎバルーニング・モードのベータ値限界は$g_T=3.3$の値を保つ（g_T：Troyon係数）。不安定なｎ＝１モードは，$q_0>1.0$の場合，プラズマ周辺に強く局在し（ピーリング・モード），そのベータ値限界は$g_T=3.7$である。$q_0<0.9$の場合，ｎ＝１モードの安定性は内部キンク・モードで決まり，$q_0=0.8$でベータ値限界は$g_T=2.4$に減少する。この安定性解析によってq_0を0.9以上に保ち，かつ，プラズマ周辺の電流分布を固定すれば$g_T=3.0$のＨ－モード分布が実現され得ることが示された。また，この解析において，ＴＡＣ－４ Ｈ－モード分布の安定性はプラズマ周辺の電流分布に敏感であることもわかった。

那珂研究所：〒311-01 茨城県那珂郡那珂町大字向山801-1

Contents

目次

1. Introduction

Long pulse operation of ITER with the high confinement mode such as H–mode plays a crucial role in assuring the performance of ITER as an experimental reactor. There are many issues to be clarified in MHD stability analyses of H–mode plasmas when compared with L–mode plasmas. Besides the assessment of the attainable beta (beta limit) for the pressure and current density profiles as in the case of the L–mode profiles, MHD stability analysis is required to study the edge localized modes (ELMs) which limit the edge density and temperature [1]. The evaluation is also desired for the influence of ELMs on the global beta limit. However, difficulties arise in the analysis of the ELMs. They strongly depend on both the edge safety factor, q_{edge}, and on the pressure and current density profiles near the plasma edge. Experiments show that the plasma surface for q_{edge} is different from the outermost equilibrium flux surface [2]. Such a surface will be different among devices. Therefore, the ELMs analysis needs the detailed information about the profiles and the edge q-values in experiments or in a well established model.

In this paper we investigate the MHD stability properties of the ITER TAC4 H–mode profiles. We will restrict ourselves to the analyses on the effects of the current profile variations on the stability of high-n ballooning modes and the n = 1 mode (n: toroidal mode number) as in the analysis of the L–mode profiles [3]. By these analyses we assess the beta limit of these modes for the TAC4 H–mode profiles. We vary the current profile without changing the total plasma current. Such a variation is characterized by the value of the safety factor on the magnetic axis, q_0. The q_{edge} value is determined only by the beta value.

In Sec. 2 we numerically analyze the MHD equilibria with the given H–mode profiles by using the MEUDAS equilibrium code which is adapted to use the profile data. In Sec. 3 we investigate the stability of the high-n ballooning modes and the n = 1 mode and consequently obtain the stability diagram of the equilibria with TAC4 H–mode profiles. Conclusions are given in Sec. 4.

2. Adaptation of the MEUDAS Equilibrium Code

The MEUDAS code has been adapted to analyze the equilibria with aids of profile data because it is difficult to make functional fittings which adjust the H–mode profiles. In the present work it is convenient to construct the MHD equilibria from the profiles of p' and surface averaged current density J = <j·**B**>/(R_{maj}<**B**·φ>), where R_{maj} is the major radius, φ is the toroidal angle, and <...> denotes the surface average, respectively. In the MEUDAS code, p' and J are expressed as

$$p'(\Psi) = -c_p F_p(\Psi) , \tag{1}$$

$$J(\Psi) = c_J F_J(\Psi) S(\Psi) , \tag{2}$$

where Ψ is the normalized poloidal flux label and $F_p(\Psi)$ and $F_J(\Psi)$ are the profile functions, as shown in Fig. 1. Coefficients c_p and c_J in Eqs. (1) and (2) are determined in such a way that the poloidal beta β_J and total plasma current Ip take the prescribed values. The function S(Ψ) is used for the current profile variations and is chosen as

$$S(\Psi) = 1 + \alpha \exp[-(\frac{\Psi}{w})^2] . \tag{3}$$

Here the coefficient α is adjusted so that q_0 takes a given value. The width w is chosen as w = 0.2, for which ρ(q=1)/a ~ 0.6 in case of q_0 = 0.8, where ρ(q=1) is the radius of the q = 1 surface and a is the plasma radius. Figure 2 illustrates the flux contours ψ(r,z) (Fig. 2(a)) and the profile of safety factor q (Fig. 2(b)) for β_J = 1.0 and Ip = 25MA ($S(\Psi) \equiv 1$). As shown in Fig. 2(b), the safety factor obtained from the MEUDAS code (solid line) is in good agreement with the one given for the TAC4 H–mode profile (dotted line).

In the present work the effects of q_0 on the MHD stability are mainly analyzed. Figure 3 shows the three different current profiles (Fig. 3(a)) given by Eq. (2) and the corresponding q profiles for β_J = 1.0 (Fig. 3(b)). The total plasma current Ip is fixed at the same value for these current profiles. Consequently, the value of q_{edge} changes little for the equilibria with the different current profiles but with the same value of β_J. The pressure is raised by increasing c_p in Eq.(1) and the stability of the high-n ballooning modes and the n=1 mode is analyzed. In the present work the 97.5 % equilibrium flux surface is adopted as the "plasma surface" for the MHD stability analysis because the safety factor on this surface is closer to the "effective edge safety factor" [2] than one on the 95% surface. The value of q_{edge} changes with the increase in β_J and lies in a range $3 < q_{edge} < 4$ for the values of β_J and q_0 of the equilibria studied here.

3. MHD Stability Properties of the H-mode Profiles

When the pressure increases with keeping the same pressure profile, the high-n ballooning modes become unstable near the region of $\Psi = 0.6$. When the pressure increases further, the edge region enters into the unstable region. The beta limit of these modes is $g_T = 3.3$, where g_T is Troyon's factor (normalized beta) defined by

$$g_T = \beta(\%) \frac{a(m)\ B_0(T)}{Ip(MA)} \ .$$

The beta limit of the high-n ballooning modes is not affected by q_0 because $p' \approx 0$ near the magnetic axis.

The stability of the n = 1 mode is studied by using the JAERI ERATO code with a boundary condition of a wall located at infinity. Figure 4 shows the g_T dependence of the squared growth rate γ^2 of the n = 1 mode in cases of (a) $q_0 = 1.0$ and 0.9, and (b) $q_0 = 0.85$ and 0.8. In Fig. 4(a) the growth rate does not show monotonic increase with g_T. On the other hand, there is a region in g_T where γ^2 remains small values of order $10^{-4} \sim 10^{-5}$ in Fig. 4(b).

In Fig. 5(a) the poloidal harmonics Xm(s) of $X(s, \theta) = \xi \bullet \nabla \psi$ are shown, where ξ is the displacement vector of the unstable n= 1 mode for $q_0 = 1.0$ and $g_T = 4.1$ ($s= \sqrt{\Psi}$), and in Fig. 5(b) the potential energy distribution of the mode is shown. The green line with the symbol "+" denotes the kink term, the blue line with the symbol "o" the ballooning term and the red line with the symbol "•" the total potential energy Wp. It is found that the current driven external kink mode is strongly localized near the plasma edge (peeling mode) [4,5] and that the m = 4 harmonic is dominant in the parameter range of $3 < q_{edge} < 4$. The growth rate of such a mode strongly depends on both raised by increasing c_p in Eq.(1) and the stability of the high-n ballooning modes and the n=1 mode is analyzed. In the present work the 97.5 % equilibrium flux surface is adopted as the "plasma surface" for the MHD stability analysis because the safety factor on this surface is closer to the "effective edge safety factor" [2] than one on the 95% surface. The value of q_{edge} changes with the increase in β_J and lies in a range $3 < q_{edge} < 4$ for the values of β_J and q_0 of the equilibria studied here.

3. MHD Stability Properties of the H–mode Profiles

When the pressure increases with keeping the same pressure profile, the high-n ballooning modes become unstable near the region of $\Psi = 0.6$. When the pressure increases further, the edge region enters into the unstable region. The beta limit of these modes is $g_T = 3.3$, where g_T is Troyon's factor (normalized beta) defined by

$$g_T = \beta(\%) \frac{a(m)\ B_0(T)}{Ip(MA)} .$$

The beta limit of the high-n ballooning modes is not affected by q_0 because $p' \approx 0$ near the magnetic axis.

The stability of the n = 1 mode is studied by using the JAERI ERATO code with a boundary condition of a wall located at infinity. Figure 4 shows the g_T dependence of the squared growth rate γ^2 of the n = 1 mode in cases of (a) $q_0 = 1.0$ and 0.9, and (b) $q_0 = 0.85$ and 0.8. In Fig. 4(a) the growth rate does not show monotonic increase with g_T. On the other hand, there is a region in g_T where γ^2 remains small values of order $10^{-4} \sim 10^{-5}$ in Fig. 4(b).

In Fig. 5(a) the poloidal harmonics Xm(s) of $X(s, \theta) = \xi \bullet \nabla\psi$ are shown, where ξ is the displacement vector of the unstable n= 1 mode for $q_0 = 1.0$ and $g_T = 4.1$ ($s = \sqrt{\Psi}$), and in Fig. 5(b) the potential energy distribution of the mode is shown. The green line with the symbol "+" denotes the kink term, the blue line with the symbol "o" the ballooning term and the red line with the symbol "•" the total potential energy Wp. It is found that the current driven external kink mode is strongly localized near the plasma edge (peeling mode) [4,5] and that the m = 4 harmonic is dominant in the parameter range of $3 < q_{edge} < 4$. The growth rate of such a mode strongly depends on both

q_{edge} and the magnetic shear at the edge, which are varied with the values of g_T in the present case. This result yields the g_T dependence of the growth rate as shown in Fig. 4(a).

On the other hand, the n = 1 mode structures for $q_0 < 1$ are quite different in high and low beta cases. Figure 6 and 7 show the radial structures of Xm(s) and the potential energy distributions of the unstable modes for q_0 = 0.8 in cases of g_T = 4.5 and g_T = 3.1, respectively. The mode with g_T = 4.5 shows a peeling mode with a subdominant m = 1 harmonic which has the feature of the internal kink mode. As g_T decreases, the peeling mode is stabilized and the n = 1 mode becomes the internal kink mode with the dominant m = 1 harmonic, as shown in Fig.7, where the growth rates are smaller than those of the peeling mode. This transition from the peeling mode to the internal kink mode affects the g_T dependence of the growth rate in Fig. 4(b). The beta limits for $q_0 < 0.9$ are determined by the internal kink mode.

Figure 8 is the stability diagram for the H–mode profiles. The blue line with the symbol "o" denotes the beta limit of the high-n ballooning modes and the red line with the symbol "•" denotes that of the n = 1 mode. When $q_0 > 0.9$, for which the n = 1 mode has the feature of the peeling mode, the beta limit of this mode is g_T = 3.7 which is higher than that of the high-n ballooning modes . While $q_0 < 0.9$, the n = 1 mode close to the marginal stability has the feature of the internal kink mode and the beta limit drops to g_T = 2.4 for q_0 = 0.8.

4. Conclusions

In the present work the ideal MHD stability properties of the ITER H–mode profiles have been studied. Equilibria were numerically obtained by the MEUDAS code adapted so as to compute them for given profiles of p' and $J = \langle j \cdot \mathbf{B} \rangle / (R_{maj} \langle \mathbf{B} \cdot \nabla\varphi \rangle)$. To understand the stability of the plasmas with H–mode profiles, we analyzed the effects of the current profile variations on the MHD stability. In this study the total plasma current was fixed at the same value and thereby the change of the edge safety factor comes from the change of beta.

We obtained the stability diagram for the high-n ballooning modes and the n = 1 mode. The beta limit of the high-n ballooning modes is g_T = 3.3 for the current profile variations. The beta limit of the n = 1 mode for $q_0 > 0.9$, for which this mode has the feature of the peeling mode, is g_T = 3.7 which is

q_{edge} and the magnetic shear at the edge, which are varied with the values of g_T in the present case. This result yields the g_T dependence of the growth rate as shown in Fig. 4(a).

On the other hand, the n = 1 mode structures for $q_0 < 1$ are quite different in high and low beta cases. Figure 6 and 7 show the radial structures of Xm(s) and the potential energy distributions of the unstable modes for q_0 = 0.8 in cases of $g_T = 4.5$ and $g_T = 3.1$, respectively. The mode with $g_T = 4.5$ shows a peeling mode with a subdominant m = 1 harmonic which has the feature of the internal kink mode. As g_T decreases, the peeling mode is stabilized and the n = 1 mode becomes the internal kink mode with the dominant m = 1 harmonic, as shown in Fig.7, where the growth rates are smaller than those of the peeling mode. This transition from the peeling mode to the internal kink mode affects the g_T dependence of the growth rate in Fig. 4(b). The beta limits for $q_0 < 0.9$ are determined by the internal kink mode.

Figure 8 is the stability diagram for the H–mode profiles. The blue line with the symbol "o" denotes the beta limit of the high-n ballooning modes and the red line with the symbol "•" denotes that of the n = 1 mode. When $q_0 > 0.9$, for which the n = 1 mode has the feature of the peeling mode, the beta limit of this mode is $g_T = 3.7$ which is higher than that of the high-n ballooning modes . While $q_0 < 0.9$, the n = 1 mode close to the marginal stability has the feature of the internal kink mode and the beta limit drops to $g_T = 2.4$ for $q_0 = 0.8$.

4. Conclusions

In the present work the ideal MHD stability properties of the ITER H–mode profiles have been studied. Equilibria were numerically obtained by the MEUDAS code adapted so as to compute them for given profiles of p' and $J = \langle j \cdot \mathbf{B} \rangle / (R_{maj} \langle \mathbf{B} \cdot \nabla\varphi \rangle)$. To understand the stability of the plasmas with H–mode profiles, we analyzed the effects of the current profile variations on the MHD stability. In this study the total plasma current was fixed at the same value and thereby the change of the edge safety factor comes from the change of beta.

We obtained the stability diagram for the high-n ballooning modes and the n = 1 mode. The beta limit of the high-n ballooning modes is $g_T = 3.3$ for the current profile variations. The beta limit of the n = 1 mode for $q_0 > 0.9$, for which this mode has the feature of the peeling mode, is $g_T = 3.7$ which is

higher than that of the high-n ballooning modes. When $q_0 < 0.9$, the $n = 1$ mode shows the feature of the internal kink mode. The beta limit of this mode becomes smaller than that of the high-n ballooning modes and reduces to $g_T = 2.4$ for $q_0 = 0.8$.

In the present work, we mainly studied the effects of q_0 on the MHD stability for the H–mode profiles and did not investigate ELMs. We restricted the current profile variations so that they do not yield change of q_{edge} and set the plasma surface for MHD stability analysis at 97.5 % of the outermost equilibrium surface. However, our calculations indicates that the stability of the TAC4 H–mode profile is sensitive to the edge current profile and that the MHD stability of ELMs is to be analyzed with aids of experimental results or a well established model.

Acknowledgment

The authors wish to thank Dr. Y. Kamada for useful discussions on the MHD stability in H-mode plasmas. They also thank Drs. H. Kishimoto, M. Azumi and H. Maeda for the continuous encouragement.

References

[1] M. Kikuchi, H. Shirai, T. Takizuka, Y. Kamada, Y. Koide., et al., in *14 th International Conference on Plasma Physics and Controlled Nuclear Fusion Research,* Wurzburg, 1992 (IAEA, Vienna, 1993), Vol. 1, p.219.

[2] Y. Kamada, T. Takizuka, M. Kikuchi, and H. Ninomiya, Nucl. Fusion, **33**, 225 (1993).

[3] S. Tokuda and T. Ozeki, "Stability Analysis of External Kink Mode for ITER L–Mode Profile Plasmas," JAERI-Research 94-013 (1994).

[4] E. A. Frieman, J. M. Greene, J.L. Johnson, and K.E. Weimer, Phys. Fluids **16**, 1108 (1973).

[5] J. Manickam, Phys. Fluids B **4**, 1901 (1992).

higher than that of the high-n ballooning modes. When $q_0 < 0.9$, the $n = 1$ mode shows the feature of the internal kink mode. The beta limit of this mode becomes smaller than that of the high-n ballooning modes and reduces to $g_T = 2.4$ for $q_0 = 0.8$.

In the present work, we mainly studied the effects of q_0 on the MHD stability for the H–mode profiles and did not investigate ELMs. We restricted the current profile variations so that they do not yield change of q_{edge} and set the plasma surface for MHD stability analysis at 97.5 % of the outermost equilibrium surface. However, our calculations indicates that the stability of the TAC4 H–mode profile is sensitive to the edge current profile and that the MHD stability of ELMs is to be analyzed with aids of experimental results or a well established model.

Acknowledgment

The authors wish to thank Dr. Y. Kamada for useful discussions on the MHD stability in H-mode plasmas. They also thank Drs. H. Kishimoto, M. Azumi and H. Maeda for the continuous encouragement.

References

[1] M. Kikuchi, H. Shirai, T. Takizuka, Y. Kamada, Y. Koide., et al., in *14 th International Conference on Plasma Physics and Controlled Nuclear Fusion Research,* Wurzburg, 1992 (IAEA, Vienna, 1993), Vol. 1, p.219.

[2] Y. Kamada, T. Takizuka, M. Kikuchi, and H. Ninomiya, Nucl. Fusion, **33**, 225 (1993).

[3] S. Tokuda and T. Ozeki, "Stability Analysis of External Kink Mode for ITER L–Mode Profile Plasmas," JAERI-Research 94-013 (1994).

[4] E. A. Frieman, J. M. Greene, J.L. Johnson, and K.E. Weimer, Phys. Fluids **16**, 1108 (1973).

[5] J. Manickam, Phys. Fluids B **4**, 1901 (1992).

higher than that of the high-n ballooning modes. When $q_0 < 0.9$, the $n = 1$ mode shows the feature of the internal kink mode. The beta limit of this mode becomes smaller than that of the high-n ballooning modes and reduces to $g_T = 2.4$ for $q_0 = 0.8$.

In the present work, we mainly studied the effects of q_0 on the MHD stability for the H-mode profiles and did not investigate ELMs. We restricted the current profile variations so that they do not yield change of q_{edge} and set the plasma surface for MHD stability analysis at 97.5 % of the outermost equilibrium surface. However, our calculations indicates that the stability of the TAC4 H-mode profile is sensitive to the edge current profile and that the MHD stability of ELMs is to be analyzed with aids of experimental results or a well established model.

Acknowledgment

The authors wish to thank Dr. Y. Kamada for useful discussions on the MHD stability in H-mode plasmas. They also thank Drs. H. Kishimoto, M. Azumi and H. Maeda for the continuous encouragement.

References

[1] M. Kikuchi, H. Shirai, T. Takizuka, Y. Kamada, Y. Koide., et al., in *14 th International Conference on Plasma Physics and Controlled Nuclear Fusion Research,* Wurzburg, 1992 (IAEA, Vienna, 1993), Vol. 1, p.219.

[2] Y. Kamada, T. Takizuka, M. Kikuchi, and H. Ninomiya, Nucl. Fusion, **33**, 225 (1993).

[3] S. Tokuda and T. Ozeki, "Stability Analysis of External Kink Mode for ITER L-Mode Profile Plasmas," JAERI-Research 94-013 (1994).

[4] E. A. Frieman, J. M. Greene, J.L. Johnson, and K.E. Weimer, Phys. Fluids **16**, 1108 (1973).

[5] J. Manickam, Phys. Fluids B **4**, 1901 (1992).

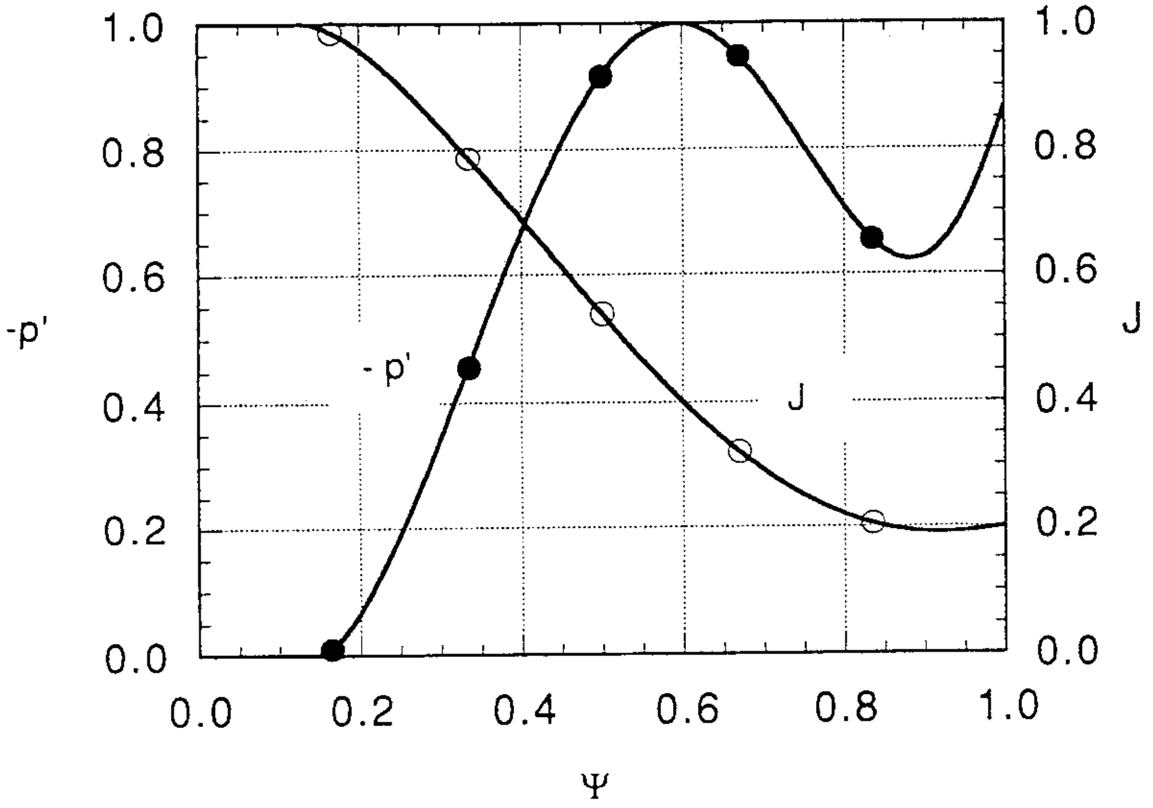

Fig.1 Profiles of p' (solid line with the symbol " • ") and the surface averaged current density J (solid line with the symbol "o") used as input data to construct equilibria with TAC4 H-mode profiles. Ψ is the normalized poloidal flux label.

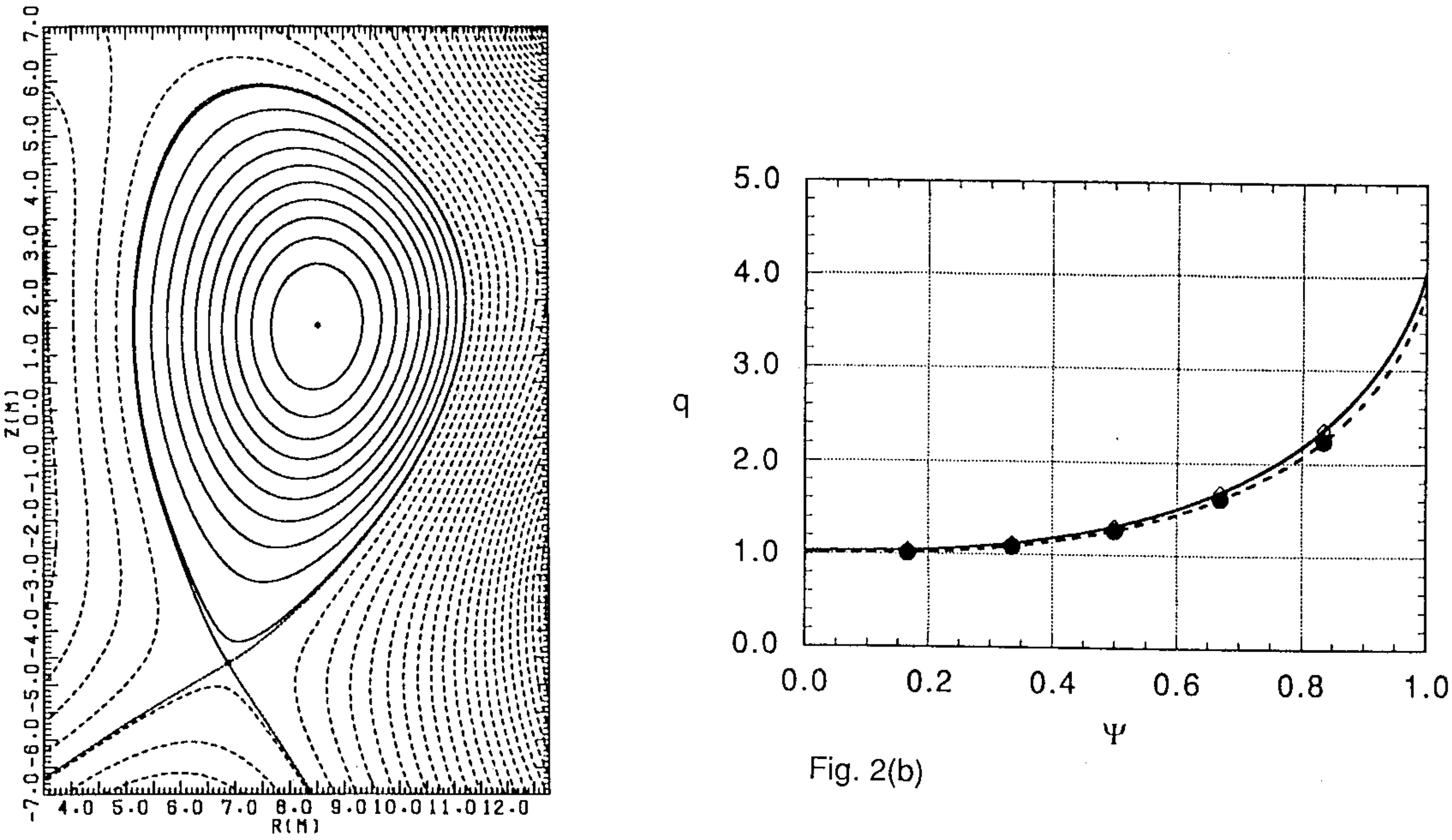

Fig. 2(a)

Fig. 2(b)

Fig.2 (a) Two dimensional flux contours $\Psi(r,z)$ and (b) safety factor $q(\Psi)$ (solid line) computed by the MEUDAS code using the profiles of p' and J given in Fig.1. The dotted line shows the q profile given as the TAC4 H-mode profile.

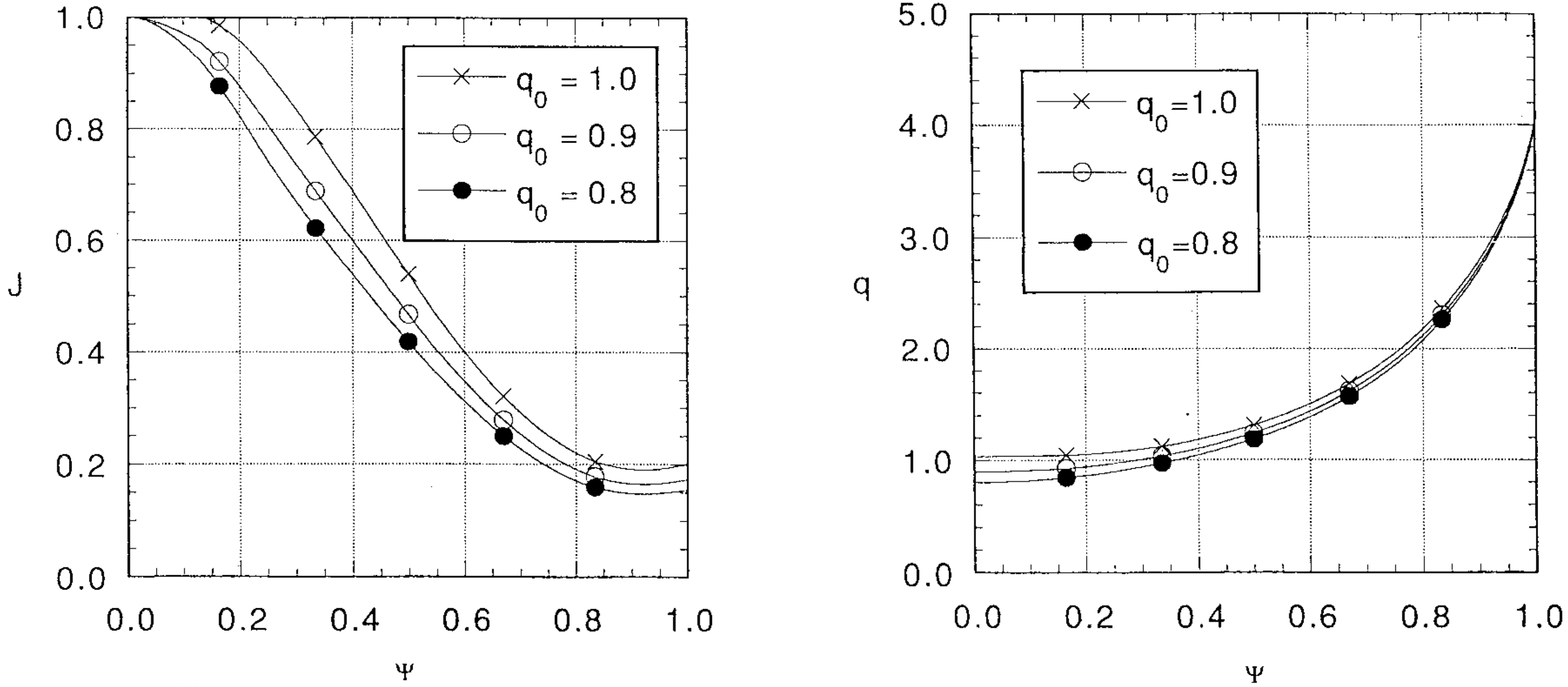

Fig. 3(a)

Fig. 3(b)

Fig.3 (a) Current density profiles J(Ψ) and (b) the corresponding q profiles obtained from the MEUDAS code for β_J=1.0. The coefficient α in Eq. (3) is adjusted so that q_0 takes a given value.

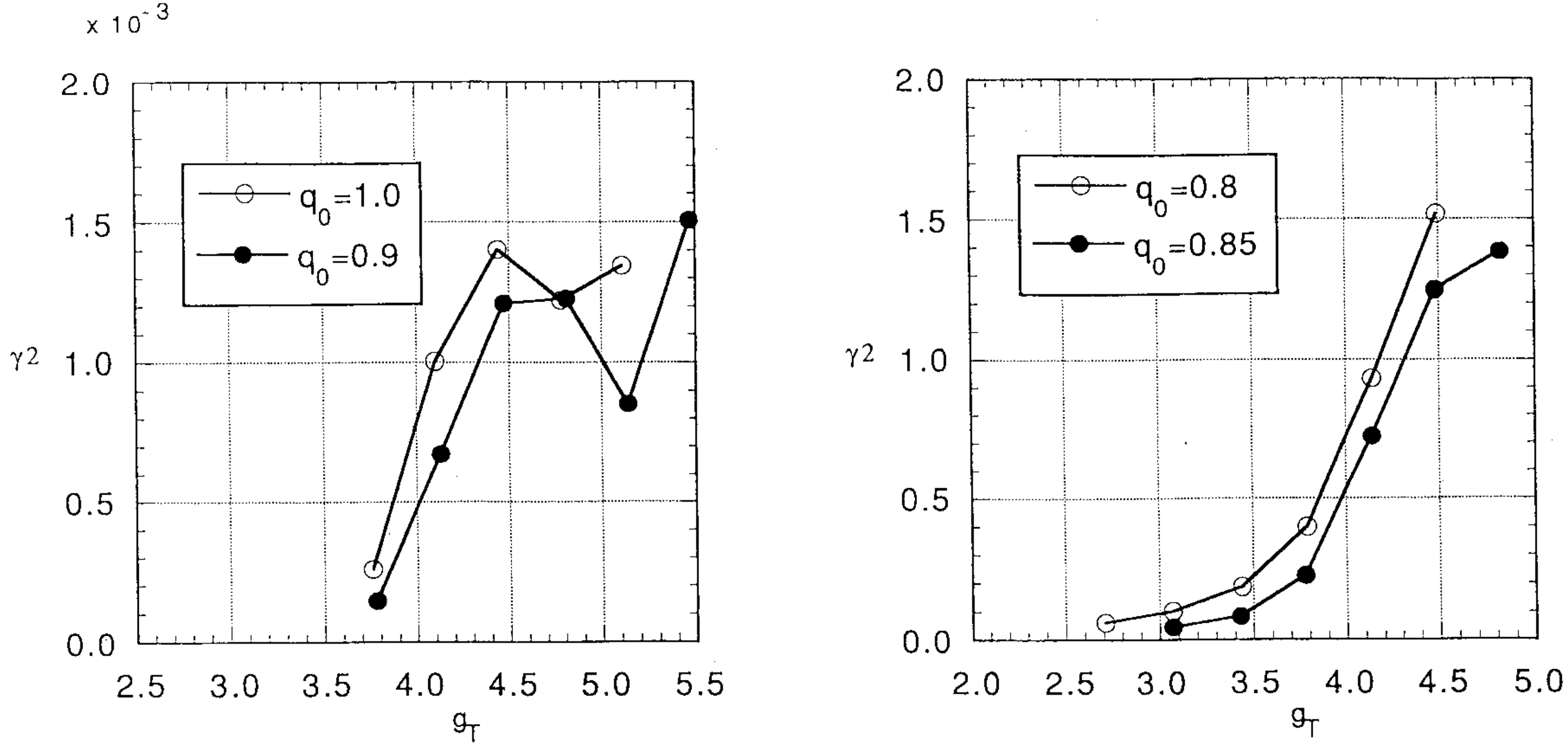

Fig. 4(a)

Fig. 4(b)

Fig.4 Dependence of the squared growth rate γ^2 on the normalized beta g_T in cases of (a) q_o=1.0 and 0.9, and (b) q_o=0.85 and 0.8

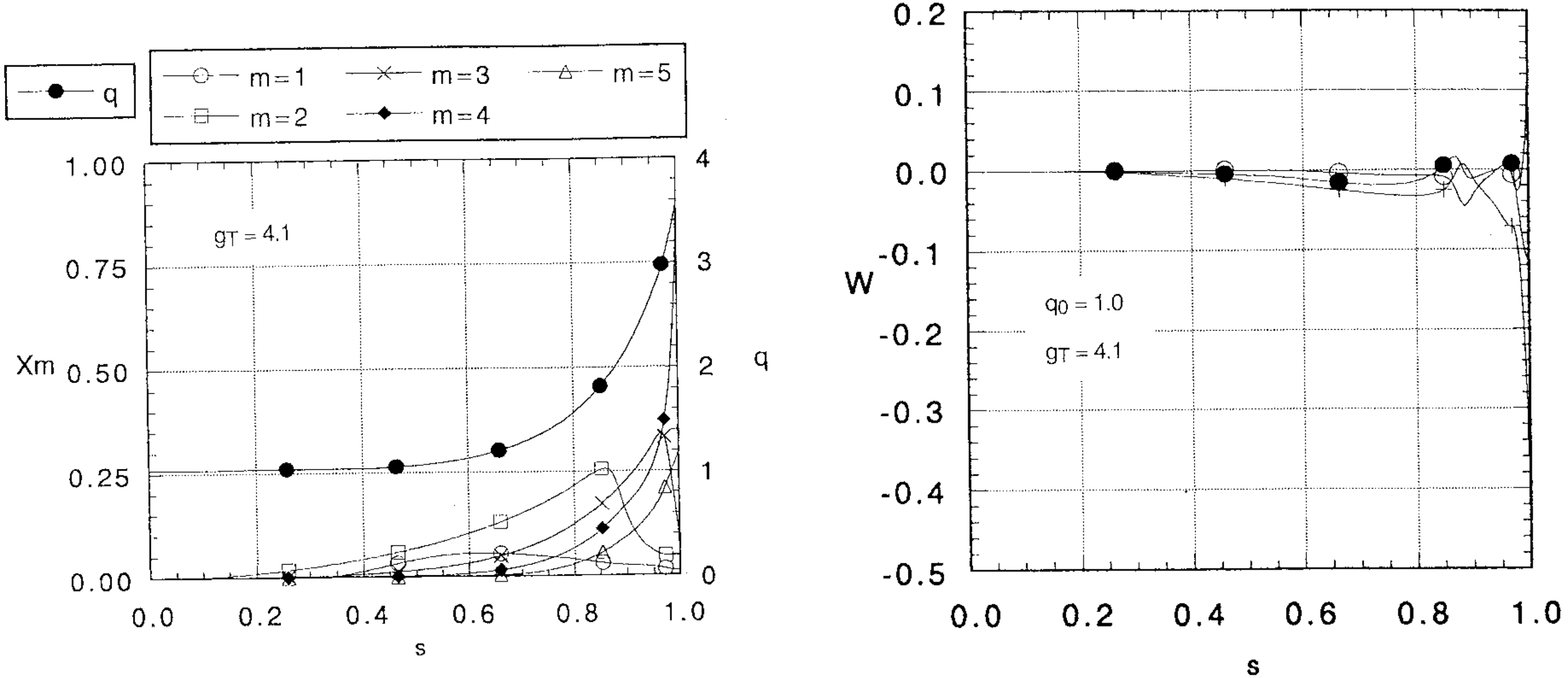

Fig. 5(a)

Fig. 5(b)

Fig.5 (a) Poloidal harmonics Xm(s) of X(s, θ)=$\xi \cdot \nabla \phi$ for $q_o=1.0$ and $g_T=4.1$ ($s=\sqrt{\Psi}$), where ξ is the displacement vector of the unstable n=1 mode.
(b) Potential energy distribution of the mode. The green line with the symbol "+" denotes the kink term, the blue line with the symblo "o" the ballooning term and the red line with the symbol "•" the total potential energy Wp.
This mode exhibits the feature of the "peeling mode" and the m=4 harmonic is dominant in the parameter range of $3<q_{edge}<4$.

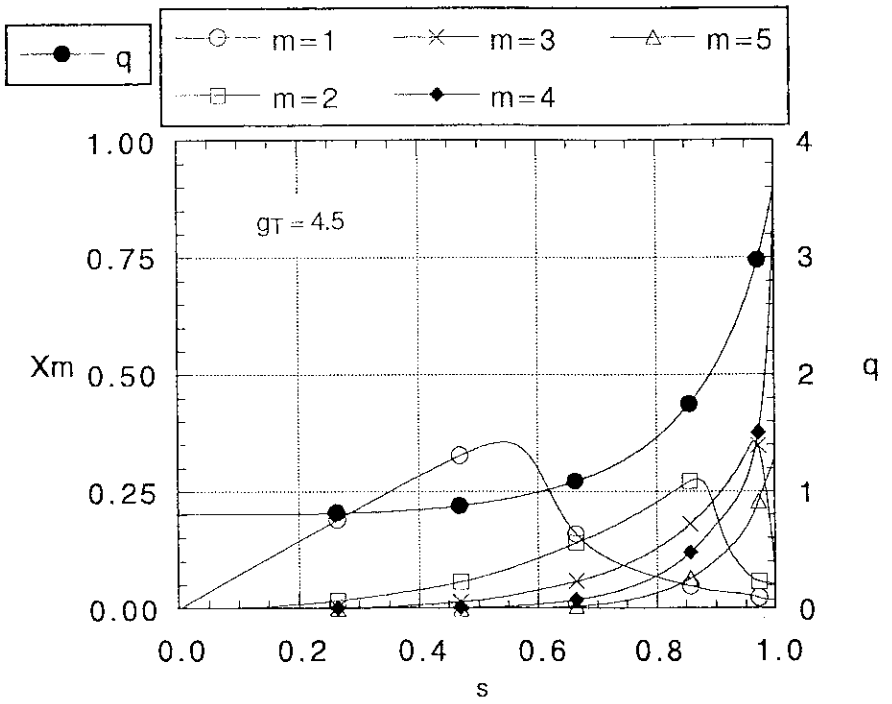

Fig. 6(a)

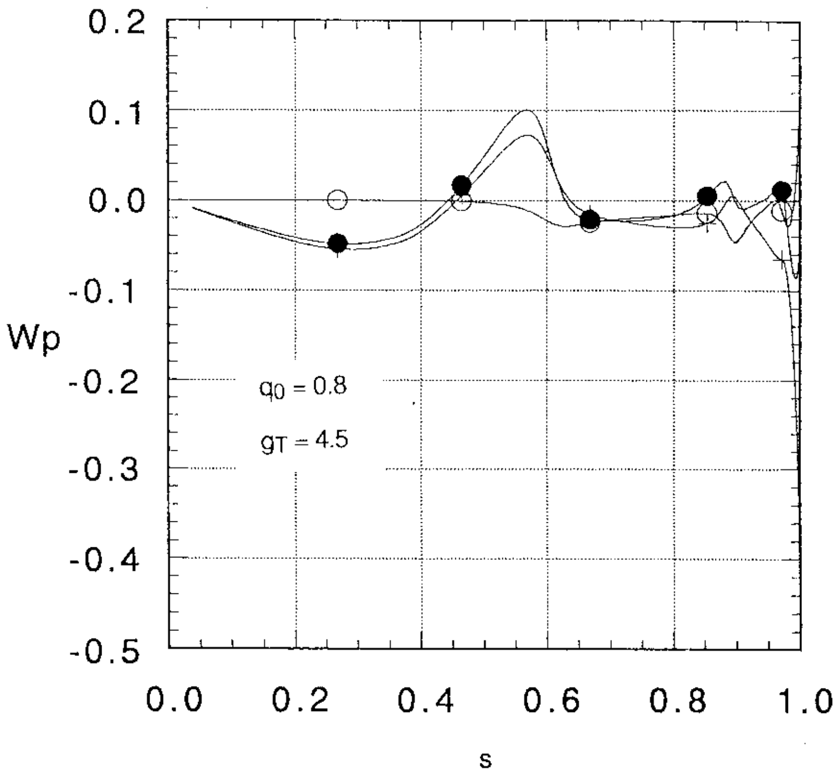

Fig. 6(b)

Fig.6 (a) Radial structure of poloidal harmonics Xm(s) and (b) potential energy distribution of the unstable n =1 mode for q_0=0.8 and g_T=4.5. The symbols in Fig.6 (b) are the same as those in Fig.5(b). The peeling mode with a subdominant m=1 harmonic appears which has the feature of the intenal kink mode.

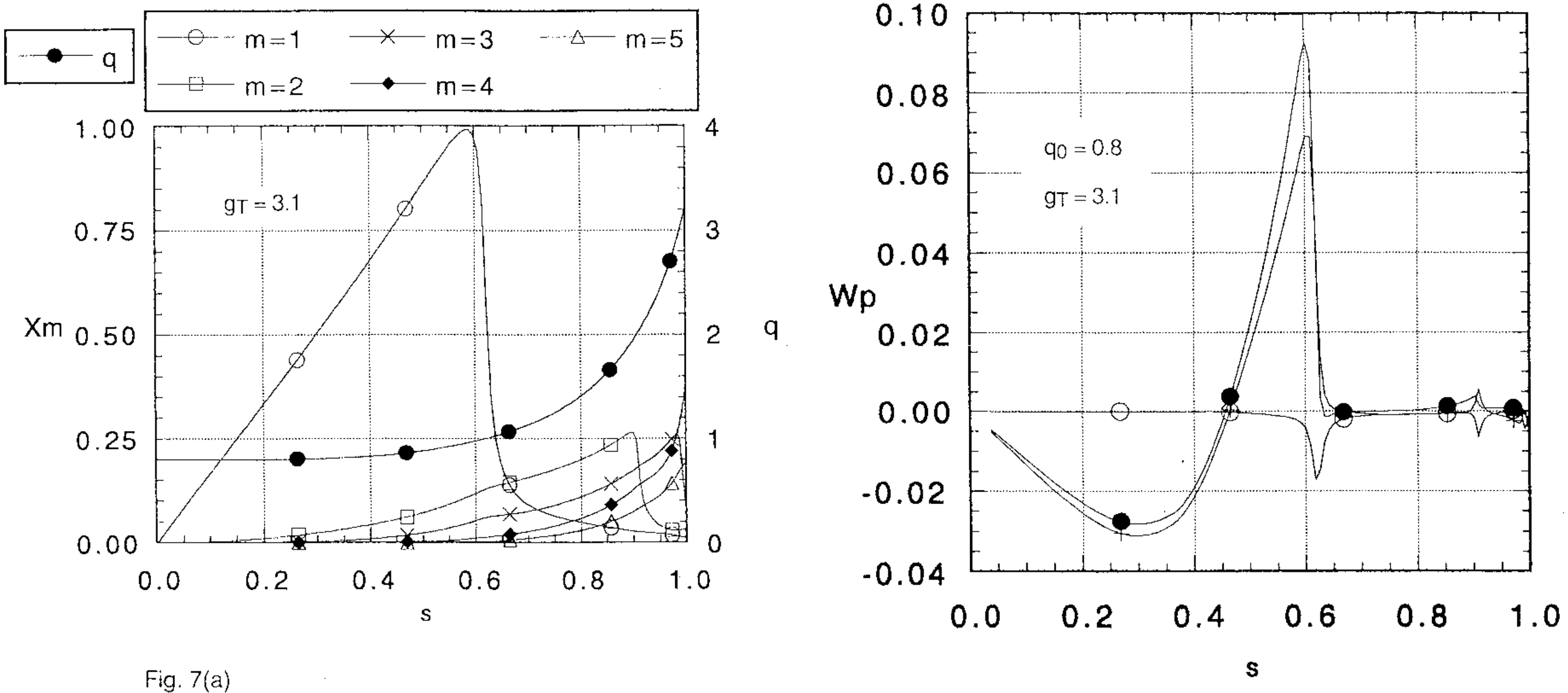

Fig. 7(a)

Fig. 7(b)

Fig.7 (a) Radial structure of poloidal harmonics Xm(s) and (b) potential energy distribution of the unstable n =1 mode for q_0=0.8 and g_T=3.1. The symbols in Fig.7(b) are the same as those in Fig.5(b).
The feature of the internal kink mode with the dominant m=1 harmonic appears. The transition from the peeling mode to the internal kink mode affects the g_T dependence of the growth rate in Fig.4(b).

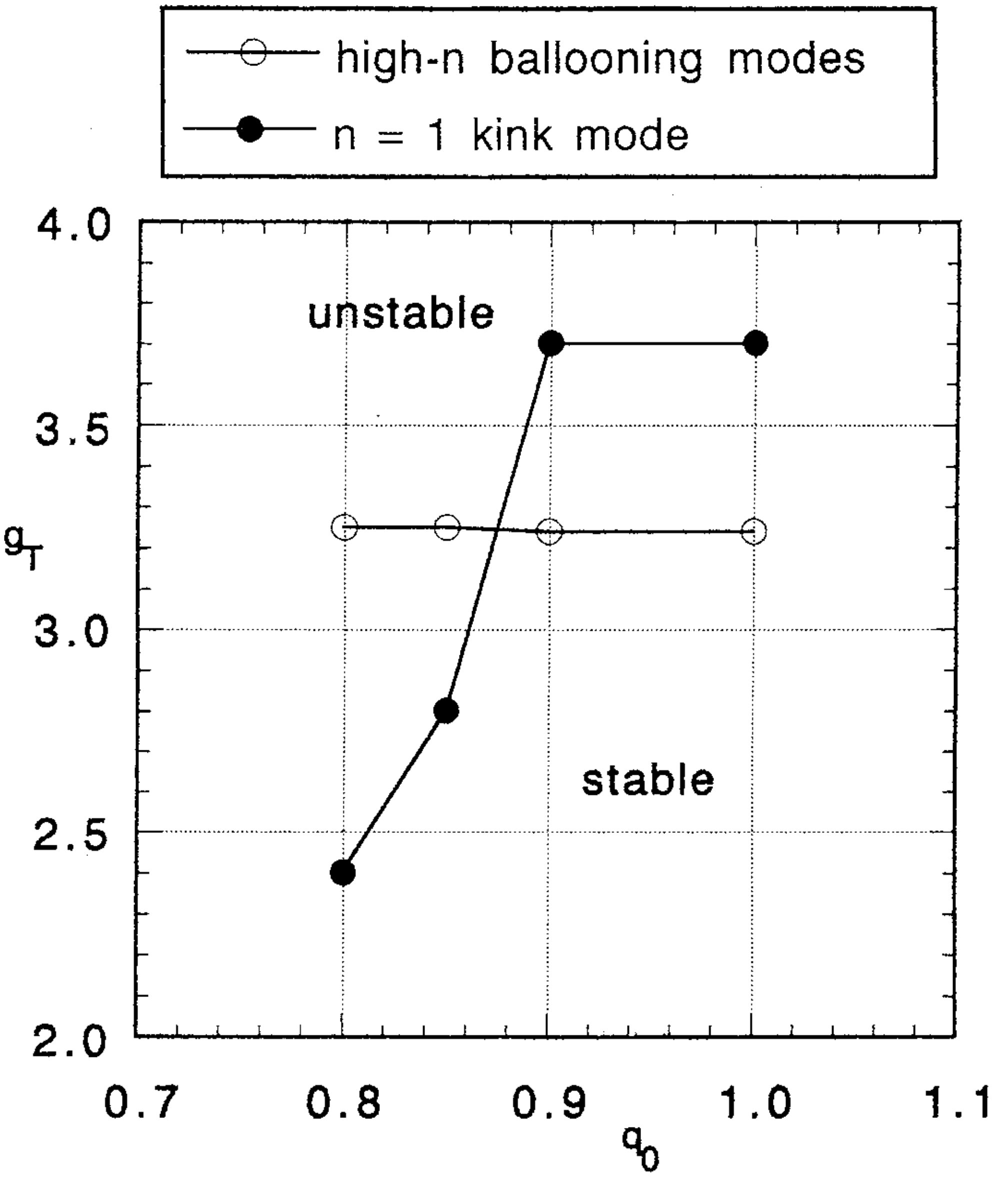

Fig.8　Stability diagram of the high-n ballooning modes and the n=1 mode for the equilibria with TAC4 H-mode profiles. The blue line with the symbol "o" indicates the high-n ballooning modes and the red line with the symbol "•" the n=1 mode. The beta limit for $q_0>0.9$ is determined by the high-n ballooning modes which becomes unstable in the middle plasma region around $\Psi=0.6$, and the internal kink mode is dominant for $q_0>0.9$.